JOURNAL OF Materials CHEMISTRY

Ternary aluminides LnT_2Al_{10} (Ln = Y, La–Nd, Sm, Gd–Lu and T = Fe, Ru, Os) with $YbFe_2Al_{10}$ type structure and magnetic properties of the iron-containing series

Verena M. T. Thiede, Thomas Ebel and Wolfgang Jeitschko

Anorganisch-Chemisches Institut, Universität Münster, Wilhelm Klemm-Strasse 8, D-48149 Münster, Germany

Of the title compounds 25 have been prepared for the first time. They crystallize with the orthorhombic $YbFe_2Al_{10}$ type structure (*Cmcm*, $Z = 4$), which was refined from single-crystal X-ray data of $SmFe_2Al_{10}$ [$a = 898.9(2)$, $b = 1018.6(2)$, $c = 904.3(2)$ pm, $R = 0.043$ for 823 structure factors and 19 variable parameters] and $LaOs_2Al_{10}$ [$a = 920.5(6)$, $b = 1027.4(5)$, $c = 916.9(6)$ pm, $R = 0.047$ for 1475 F values and 21 variables]. Two aluminium sites of $LaOs_2Al_{10}$ show significant deviations from the ideal occupancies, resulting in the exact composition $LaOs_2Al_{9.74(2)}$. The magnetic properties of the iron-containing compounds have been determined with a SQUID magnetometer in the temperature range 2–300 K with magnetic flux densities up to 5.5 T. YFe_2Al_{10} and $LaFe_2Al_{10}$ are Pauli-paramagnetic, indicating that the iron atoms in these isotypic compounds do not carry magnetic moments. The behaviour of the other iron-containing compounds is dominated by the magnetic properties of the rare-earth components. $CeFe_2Al_{10}$ and $YbFe_2Al_{10}$ show mixed-valent behaviour. This can also be concluded from the cell volumes for $CeRu_2Al_{10}$ and $YbRu_2Al_{10}$. $SmFe_2Al_{10}$ is Van Vleck paramagnetic, and the others follow the Curie–Weiss law with magnetic ordering temperatures of <20 K. The magnetic properties of these compounds were further investigated by magnetization measurements at 2 K.

A large number of ternary aluminides containing the lanthanoids and iron have been synthesized in recent years, because of their interesting magnetic properties. Many of these aluminides crystallize with ordered variants of binary structure types. The series $LnFe_4Al_8$ (Ln = La–Lu) has a structure, first determined for $CeMn_4Al_8$, where the transition metals and aluminium occupy different atomic sites of the $ThMn_{12}$-type structure.[1–8] The structure of the series $LnFe_6Al_6$ also derives from $ThMn_{12}$, however, in that series one manganese site has a mixed occupancy with iron and aluminium atoms.[9,10] Other ternary lanthanoid iron aluminides have been reported with crystal structures, where the iron and aluminium atoms occupy certain atomic sites of the binary $MgCu_2$, $CeNi_3$, $NaZn_{13}$, Th_2Ni_{17} and Th_2Zn_{17} structure types.[11]

Recently the new compound $YbFe_2Al_{10}$ has been characterized. Its crystal structure is of a new type, which is also related to the structure of $ThMn_{12}$, however, in contrast to the examples cited above, it is not a simple substitution variant of a binary structure type, but an orthorhombic stacking variant of the tetragonal $ThMn_{12}$ structure with a doubled c axis.[12] Compounds with the compositions $LnFe_2Al_{10}$ (Ln = Y, La–Sm, Gd, Dy–Er) have been found during phase diagram studies of the corresponding ternary systems and designated as ψ' phases, but their crystal structure has not been established.[13–22] Here we report 28 aluminides with $YbFe_2Al_{10}$ type structure. Some of the iron-containing compounds and all of the ruthenium and osmium compounds with the exception of $CeRu_2Al_{10}$[23] are characterized here for the first time. We have also investigated the magnetic properties of the iron-containing compounds.

Experimental

Sample preparation and lattice constants

Starting materials were powders of iron (Ventron, >99.5%), ruthenium (Heraeus, >99.9%) and osmium (Alfa, >99.9%). The rare-earth elements (Kelpin, >99.9%) and aluminium (Merck, >99.9%) were purchased as ingots. Aluminium and the heavy lanthanoids were used in the form of turnings. Filings of the light lanthanoids were prepared under dried (Na) paraffin oil. The paraffin was washed out with dried hexane, and the hexane was removed under vacuum. Most samples were prepared in the atomic ratio Ln : T : Al = 1 : 2 : 12 in an alumina crucible under argon, which was sealed in a silica tube, annealed for 400 h at 800 °C and subsequently cooled at a rate of 6 °C h^{-1}. The aluminium matrix was removed by treating the products with diluted hydrochloric acid, which attacks the crystals of the ternary aluminides at a slower rate.

The energy dispersive X-ray fluorescence analyses of these crystals in a scanning electron microscope showed no impurities of elements with atomic numbers equal to or greater than sodium.

The samples were characterized by their Guinier powder patterns using Cu-Kα_1 radiation with α-quartz ($a = 491.30$, $c = 540.46$ pm) as an internal standard. The lattice constants (Table 1) were refined by least-squares fits.

Structure refinements of $SmFe_2Al_{10}$ and $LaOs_2Al_{10}$

Single crystals of $SmFe_2Al_{10}$ and $LaOs_2Al_{10}$ were mounted on a quartz fibre and intensity data were recorded on a four-circle diffractometer (Enraf-Nonius, CAD4) with graphite-monochromated Mo-Kα radiation and a scintillation counter with pulse-height discriminator. The background counts were taken at both ends of each θ–2θ scan. Absorption corrections were made from ψ scans. Further crystallographic data are summarized in Table 2.

For the structure refinements by a full-matrix least-squares program the starting parameters were taken from the $YbFe_2Al_{10}$ structure.[12] Atomic scattering factors[24] were used, corrected for anomalous dispersion.[25] Parameters accounting for isotropic secondary extinction were refined. The weighting schemes included a term, which accounted for the counting statistics. All atomic positions were refined with isotropic displacement parameters. To check for deviations from the ideal compositions, occupancy parameters were varied in one

Table 1 Lattice constants of aluminides with the orthorhombic $YbFe_2Al_{10}$-type structure[a]

compound	a/pm	b/pm	c/pm	V/nm^3
YFe_2Al_{10}	896.9(3)	1015.6(4)	901.8(3)	0.8214
$LaFe_2Al_{10}$	905.1(2)	1024.9(4)	912.2(3)	0.8461
$CeFe_2Al_{10}$[b]	894	1022	906	0.8278
$CeFe_2Al_{10}$	900.2(2)	1022.2(2)	907.3(2)	0.8348
$PrFe_2Al_{10}$	901.7(1)	1021.4(2)	908.0(1)	0.8363
$NdFe_2Al_{10}$	900.6(1)	1020.6(2)	906.9(1)	0.8335
$SmFe_2Al_{10}$	898.9(2)	1018.6(2)	904.3(2)	0.8280
$GdFe_2Al_{10}$	897.0(3)	1016.2(4)	902.3(3)	0.8229
$TbFe_2Al_{10}$	896.3(3)	1014.9(4)	901.3(3)	0.8199
$DyFe_2Al_{10}$	895.4(2)	1014.1(2)	900.0(2)	0.8172
$HoFe_2Al_{10}$	895.3(2)	1013.7(4)	899.7(3)	0.8165
$ErFe_2Al_{10}$	895.8(3)	1013.6(3)	898.8(2)	0.8162
$TmFe_2Al_{10}$	895.5(2)	1012.7(2)	898.2(2)	0.8145
$YbFe_2Al_{10}$[b]	896.6(1)	1015.3(2)	900.3(1)	0.8196
$YbFe_2Al_{10}$	896.2(2)	1014.4(1)	899.3(2)	0.8175
$LuFe_2Al_{10}$	894.9(3)	1011.4(3)	898.0(3)	0.8128
YRu_2Al_{10}	912.2(3)	1021.1(4)	908.7(3)	0.8464
$LaRu_2Al_{10}$	921.4(2)	1030.0(3)	915.6(2)	0.8690
$CeRu_2Al_{10}$[b]	918.4(2)	1028.0(3)	912.5(2)	0.8615
$CeRu_2Al_{10}$	917.3(3)	1027.2(4)	912.5(3)	0.8558
$PrRu_2Al_{10}$	917.6(2)	1026.7(3)	912.1(2)	0.8593
$NdRu_2Al_{10}$	915.2(3)	1026.1(4)	911.5(3)	0.8559
$SmRu_2Al_{10}$	914.4(2)	1023.8(2)	909.5(1)	0.8515
$GdRu_2Al_{10}$	913.6(3)	1021.1(4)	909.0(3)	0.8480
$TbRu_2Al_{10}$	911.5(3)	1021.2(4)	908.5(3)	0.8456
$HoRu_2Al_{10}$	911.2(4)	1019.4(4)	908.3(3)	0.8437
$ErRu_2Al_{10}$	909.1(3)	1018.5(4)	908.3(2)	0.8410
$YbRu_2Al_{10}$	910.2(4)	1021.4(4)	908.3(4)	0.8445
$LaOs_2Al_{10}$	920.5(6)	1027.4(5)	916.9(6)	0.8672
$PrOs_2Al_{10}$	918.1(3)	1026.2(3)	915.2(3)	0.8624
$NdOs_2Al_{10}$	917.0(3)	1022.7(3)	913.8(3)	0.8570

[a]Standard deviations in the values of the last listed digits are given in parentheses throughout the crystallographic part of the paper. [b]Lattice constants from ref. 21 ($CeFe_2Al_{10}$), 23 ($CeRu_2Al_{10}$) and 12 ($YbFe_2Al_{10}$).

series of least-squares cycles together with variable thermal parameters and a fixed scale factor. For $SmFe_2Al_{10}$ the occupancy factors varied between 95.7(5)% for the Al(5) position and 101.2(6)% for the Al(3) position. These deviations were not considered to be important and for the final refinement cycles the ideal occupancy values were assumed. The refinement of the $LaOs_2Al_{10}$ data showed more significant deviations from the full occupancies for the Al(3) and Al(4) positions. Therefore, these positions were allowed to deviate from the full occupancy during the final least-squares cycles. This resulted in the exact formula $LaOs_2Al_{9.74(2)}$. However, since the deviations from the full occupancies are small we continue to use the ideal formula also for this compound for most purposes. Atomic coordinates and thermal parameters are summarized in Table 3. Listings of the structure factors are available from the authors. Full crystallographic details, excluding structure factors, have been deposited at the Cambridge Crystallographic Data Centre (CCDC). See Information for Authors, *J. Mater. Chem.*, 1998, Issue 1. Any request to the CCDC for this material should quote the full literature citation and the reference number 1145/67.

Table 3 Atomic coordinates and thermal parameters of $SmFe_2Al_{10}$ and $LaOs_2Al_{10-x}$[a]

atom	*Cmcm*	x	y	z	10^4B/pm^2
$SmFe_2Al_{10}$					
Sm	4c	0	0.1249(4)	1/4	0.410(7)
Fe	8d	1/4	1/4	0	0.36(2)
Al(1)	8g	0.2271(3)	0.3608(2)	1/4	0.55(4)
Al(2)	8g	0.3494(2)	0.1286(2)	1/4	0.53(4)
Al(3)	8f	0	0.1596(2)	0.5976(2)	0.52(4)
Al(4)	8f	0	0.3758(2)	0.0489(2)	0.64(4)
Al(5)	8e	0.2271(2)	0	0	0.63(4)
$LaOs_2Al_{9.74(2)}$					
La	4c	0	0.12476(5)	1/4	0.406(6)
Os	8d	1/4	1/4	0	0.248(2)
Al(1)	8g	0.2233(2)	0.3651(2)	1/4	0.47(3)
Al(2)	8g	0.3507(2)	0.1316(2)	1/4	0.51(3)
Al(3)[a]	8f	0	0.1624(2)	0.6023(2)	0.30(3)
Al(4)[a]	8f	0	0.3776(2)	0.0493(2)	0.39(3)
Al(5)	8e	0.2262(2)	0	0	0.55(3)

[a]The occupancy values of the Al(3) and Al(4) atoms of $LaOs_2Al_{10}$ were refined to 93.9(6) and 93.2(6) %, respectively.

SQUID magnetometry

Susceptibility measurements of powdered samples were carried out in the temperature range 2–300 K with a SQUID magnetometer (Quantum Design, Inc.) with magnetic flux densities of up to 5.5 T as described previously.[26,27] The Guinier powder diffractograms had shown no impurity phases, however, the susceptibilities of the samples of YFe_2Al_{10}, $LaFe_2Al_{10}$, $PrFe_2Al_{10}$ and $SmFe_2Al_{10}$ were field dependent above 100 K, indicating minor amounts of ferromagnetic impurities. Extrapolations of these data to infinite field strengths were not necessary since the susceptibilities determined at 3 and 5 T were already identical.

Table 2 Crystal data for $SmFe_2Al_{10}$ and $LaOs_2Al_{10-x}$

	$SmFe_2Al_{10}$	$LaOs_2Al_{9.74(2)}$
structure type	$YbFe_2Al_{10}$	$YbFe_2Al_{10}$
space group (no.)	*Cmcm* (63)	*Cmcm* (63)
lattice constants from powder [and single-crystal] data		
a/pm	898.9(2) [899.0(1)]	920.5(6) [921.4(1)]
b/pm	1018.6(2) [1018.6(1)]	1027.4(5) [1028.5(2)]
c/pm	904.3(2) [904.5(2)]	916.9(6) [917.2(2)]
V/nm^3	0.8280(2) [0.8283(2)]	0.8672(2) [0.8692(3)]
formula units per cell, Z	4	4
formula mass	531.9	782.1
D_c/g cm^{-3}	4.27	5.99
crystal dimensions/μm	$22 \times 22 \times 100$	$22 \times 22 \times 88$
$2\theta_{max}$ for θ–2θ scans/°	70	70
range in h, k, l	± 14, ± 16, ± 14	± 16, ± 18, 0–16
total number of reflections	7266	6793
highest/lowest transmission	1.48	1.37
unique reflections	1052	1533
inner residual, R_i	0.030	0.032
reflections with $I_o > 3\sigma(I_o)$	823	1475
number of variables	19	21
conventional residual, R	0.043	0.047
weighted residual, R_w	0.056	0.026

Results and Discussion

The crystals of the new compounds have silvery metallic lustre. They are not as readily attacked by dilute hydrochloric acid as the aluminium matrix. With concentrated nitric acid they are passivated as is known for elemental aluminium. They are brittle and easily ground to fine powders.

The plots of the cell volumes (Fig. 1) indicate mixed or intermediate valence for the cerium and ytterbium compounds, as is well known for many other intermetallic compounds of cerium, europium and ytterbium. For pure tetravalent cerium and divalent ytterbium greater deviations from the smooth cell volume plots could be expected. We have not been successful in preparing $EuFe_2Al_{10}$ and $EuRu_2Al_{10}$, probably because of the preference of europium for the divalent state. Several attempts were needed to prepare the $LnRu_2Al_{10}$ compounds with the heavy rare earth elements and most of these compounds were not obtained in pure form. It seems possible that these compounds have considerable deviations from the ideal composition. This is especially suggested by the unevenness of the volume plot for these compounds. We also note, that for both series $LnFe_2Al_{10}$ and $LnRu_2Al_{10}$ the lanthanoid contraction is less pronounced for the compounds with the heavy lanthanoids, and this may also be attributed to deviations from the ideal composition, as we have observed for $LaOs_2Al_{9.74}$. Such deviations also allow us to rationalize why $LaOs_2Al_{10}$ has a smaller cell volume than $LaRu_2Al_{10}$. The inverse is found for the praseodymium and neodymium compounds of the osmium and ruthenium series. Several attempts were made to prepare the missing $LnRu_2Al_{10}$ compounds with Ln = Dy, Tm and Lu. These samples showed Guinier powder patterns of another ternary phase with as yet undetermined structure. Nevertheless, we think that these compounds can probably be obtained with different atomic starting ratios.

The structure refinements of $SmFe_2Al_{10}$ and $LaOs_2Al_{10}$ prove the complete isotypy of the new aluminides with the structure previously established[12] for $YbFe_2Al_{10}$. Even the thermal parameters are similar; the smallest being those of the transition metal atoms. Remarkable exceptions are the deviations from the full occupancies for the Al(3) and Al(4) positions in the osmium compound, resulting in the composition $LaOs_2Al_{9.74(2)}$. These occupancy parameters were refined together with the isotropic displacement parameters of these atoms. We note that these displacement parameters are rather small, however, we obtained significant deviations from the full occupancies for the Al(3) and Al(4) positions of this compound also when the displacement parameters were fixed at reasonable higher values.

The interatomic distances of $SmFe_2Al_{10}$ and $LaOs_2Al_{10}$ (Table 4) reflect the smaller cell constants of $SmFe_2Al_{10}$. As could be expected, the Sm—Al and Fe—Al distances are shorter than the corresponding La—Al and Os—Al distances.

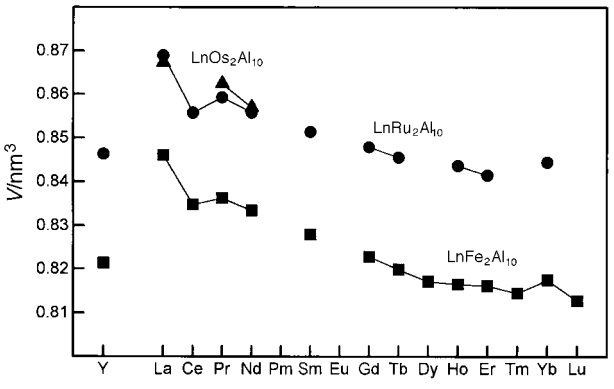

Fig. 1 Cell volumes of the aluminides $LnFe_2Al_{10}$, $LnRu_2Al_{10}$ and $LnOs_2Al_{10}$

Table 4 Interatomic distances (pm) in the structures of $SmFe_2Al_{10}/LaOs_2Al_{10}$[a]

Sm/La:	2Al(4)	313.6/318.3	Al(3):	2Fe/Os	258.4/264.3
	2Al(2)	314.1/322.9		1Al(4)	256.9/261.1
	2Al(1)	315.3/321.3		2Al(5)	275.5/282.9
	2Al(3)	316.3/324.7		1Al(3)	275.7/270.8
	2Al(3)	320.9/325.4		2Al(1)	282.1/289.8
	4Al(5)	330.1/335.2		2Al(2)	289.6/286.3
	2Al(1)	364.0/368.8		1Al(3)	370.0/382.9
	4Fe/Os	343.3/349.4		1Sm/La	316.3/324.7
Fe/Os:	2Al(1)	253.5/259.1		1Sm/La	320.9/325.4
	2Al(5)	255.5/257.8	Al(4):	2Fe/Os	262.4/268.7
	2Al(3)	258.4/264.3		1Al(3)	256.9/261.1
	2Al(4)	262.4/268.7		1Al(4)	268.1/267.4
	2Al(2)	272.8/275.5		2Al(1)	273.8/276.2
	2Sm/La	343.3/349.4		2Al(5)	279.6/285.3
Al(1):	2Fe/Os	253.5/259.1		2Al(2)	302.3/307.1
	1Al(2)	260.9/266.9		2Al(2)	343.1/347.7
	2Al(5)	270.0/271.9		1Al(4)	363.7/368.0
	2Al(4)	273.8/276.2		1Sm/La	313.6/318.3
	1Al(2)	281.3/282.2	Al(5):	2Fe/Os	255.5/257.8
	2Al(3)	282.1/289.8		2Al(1)	270.0/271.9
	1Sm/La	315.3/321.3		2Al(3)	275.5/282.9
	1Sm/La	364.0/368.8		2Al(4)	279.6/285.3
Al(2):	2Fe/Os	272.8/275.5		2Al(2)	283.5/289.8
	1Al(1)	260.9/266.9		2Sm/Os	330.1/335.2
	1Al(2)	270.7/274.8			
	1Al(1)	281.3/282.2			
	2Al(5)	283.5/289.8			
	2Al(3)	289.6/286.3			
	2Al(4)	302.3/307.1			
	2Al(4)	343.1/347.7			
	1Sm/La	314.1/322.9			

[a]All distances <400 pm are listed. The standard deviations are all $\leqslant 0.3$ pm.

Somewhat surprisingly, however, the corresponding Al—Al distances show the same tendency. They are almost always greater [with the exceptions of one Al(2)—Al(3), one Al(3)—Al(3) and one Al(4)—Al(4) distance] in the lanthanum osmium compound. Nevertheless, the Al—Al interactions are bonding. The eight shortest Al—Al distances of each aluminium coordination of both compounds cover the range 256.9–307.1 pm. This range compares favourably with the Al—Al distance of 286.3 pm in the cubic close-packed structure of elemental aluminium.[28]

The crystal structure (Fig. 2) and the coordination polyhedra of the $YbFe_2Al_{10}$ type structure have been discussed before.[12] In view of the magnetic properties, the distances between the rare earth atoms are of some importance. The coordination polyhedron of the lanthanoid atoms (Fig. 3) contains 16 aluminium and 4 transition metal atoms. There are no direct

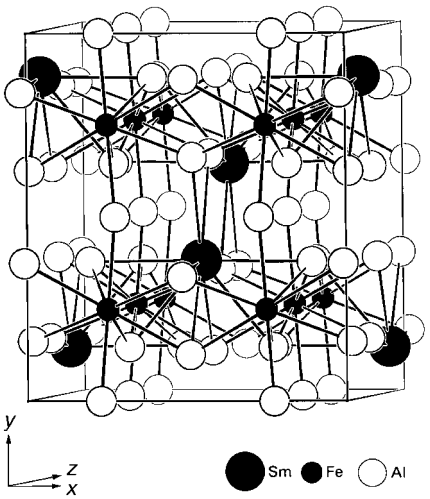

Fig. 2 The $YbFe_2Al_{10}$ type structure of $SmFe_2Al_{10}$

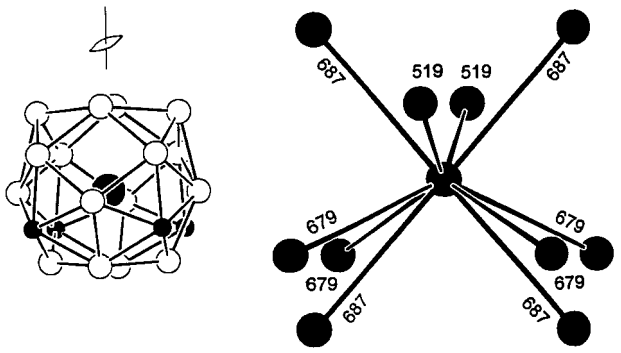

Fig. 3 Environment of a samarium atom in the structure of $SmFe_2Al_{10}$. In the coordination polyhedron on the left-hand side all near-neighbours up to 400 pm are shown. On the right-hand side only the samarium neighbours up to 800 pm are drawn.

Ln—Ln interactions. The shortest Ln—Ln distances are greater than 500 pm.

We have investigated the magnetic properties of the iron-containing compounds $LnFe_2Al_{10}$ with the exception of $LuFe_2Al_{10}$, which has not been obtained in pure form. These properties are summarized in Table 5. The magnetic susceptibilities of YFe_2Al_{10} and $LaFe_2Al_{10}$, where the rare earth elements are not expected to carry magnetic moments, are very small with room temperature values of $(6\pm1)\times10^{-9}$ m^3 (formula unit)$^{-1}$ and $(9\pm1)\times10^{-9}$ m^3 (f.u.)$^{-1}$, respectively. They are almost temperature independent (Fig. 4), indicating Pauli paramagnetism. The upturns of the magnetic susceptibilities at low temperatures can be ascribed to very minor amounts of paramagnetic impurities or to paramagnetic surface states. The fact that YFe_2Al_{10} and $LaFe_2Al_{10}$ do not show any strong magnetic moments proves that the iron atoms in these compounds are magnetically saturated, and this can also be assumed for the other aluminides of this series.

All of the other iron-containing aluminides, with the exceptions of the cerium, samarium and the ytterbium compounds, show Curie–Weiss behaviour above 50 K (Fig. 4). The magnetic moments μ_{exp}, calculated from the straight portions of the $1/\chi$ *vs.* T plots, correspond to the effective magnetic moments μ_{eff} calculated for the free Ln^{3+} ions from the relation $\mu_{eff}=g[J(J+1)]^{1/2}\ \mu_B$ (Table 5), where g is the Landé factor and J is the total angular momentum number. The Weiss constants Θ are practically zero for these compounds. This indicates that the coupling of the magnetic moments is weak, and since the Ln—Ln distances are all >500 pm, it probably occurs *via* the conduction electrons.

The temperature dependence of the reciprocal magnetic susceptibility of $CeFe_2Al_{10}$ is different from the ones just discussed, and this has probably to do with the mixed or intermediate valent behaviour of this compound, as is suggested by the plot of the cell volumes (Fig. 1). Nevertheless, above 200 K the reciprocal susceptibility seems to follow the Curie–Weiss law. A Weiss constant of $\Theta=-182\pm5$ K was extrapolated from the data above 200 K. Large negative Weiss constants are formally obtained for mixed or intermediate valent cerium compounds. If we use the equation $\mu_{exp}=2.83[\chi(T-\Theta)]^{1/2}\ \mu_B$, a magnetic moment of $\mu_{exp}=2.6\pm0.1\ \mu_B$ (f.u.)$^{-1}$ results. This moment would compare well with the free ion value for Ce^{3+} of $\mu_{eff}=2.54\ \mu_B$, calculated from the formula $\mu_{eff}=g[J(J+1)]^{1/2}\ \mu_B$, however, since cerium in this compound seems to be mixed or intermediate valent, the evaluation of the susceptibility data according to the Curie–Weiss law is not proper.[30] At low temperature the magnetic susceptibilities of $CeFe_2Al_{10}$ show some discontinuities. These might possibly be due to valence fluctuations[30] and/or to minor amounts of impurities. This was not further investigated.

No definite magnetic order could be observed for $PrFe_2Al_{10}$ and $NdFe_2Al_{10}$ down to 2 K. The discontinuity in the $1/\chi$ *vs.* T plot of the neodymium compound at 30 K is possibly caused by an unknown impurity. The magnetization behaviour of $PrFe_2Al_{10}$ and $NdFe_2Al_{10}$ at 4 K did not give any indication for magnetic order.

The magnetic behaviour of $SmFe_2Al_{10}$ can be ascribed to the Van Vleck paramagnetism of the Sm^{3+} ions. The experimentally determined value of $\mu_{exp}=1.5\pm1\ \mu_B$ calculated from the susceptibility at room temperature according to $\mu_{exp}=2.83(T\chi)^{1/2}\ \mu_B$ is close to the theoretical effective moment $\mu_{eff}=1.66\ \mu_B$, calculated from Van Vleck's formula[31] for 300 K assuming a screening constant of $\sigma=34$.

The reciprocal susceptibilities of $GdFe_2Al_{10}$, $TbFe_2Al_{10}$ and $DyFe_2Al_{10}$ show minima at low field strengths (0.1 T) indicating antiferromagnetic order with Néel temperatures of $T_N=15\pm3$ K, 14 ± 3 K and 10 ± 3 K, respectively (insets of Fig. 4). Below the Néel temperatures the reciprocal susceptibilities of these compounds become field-dependent suggesting metamagnetism. This was confirmed by magnetization measurements at 2 K (Fig. 5) for $TbFe_2Al_{10}$ and $DyFe_2Al_{10}$, although a typical hysteresis loop was observed only for the terbium compound. At the highest attainable magnetic flux density of 5.5 T the magnetization curves almost reach saturation with 'saturation magnetizations' of $\mu_{exp,sm}=7.1$ and $7.0\ \mu_B$ for $TbFe_2Al_{10}$ and $DyFe_2Al_{10}$, respectively. These values are well below the theoretical ones of 9.0 and $10.0\ \mu_B$ calculated from the relation $\mu_{calc,sm}=gJ\mu_B$ as could be expected for a powder sample with random orientation of the crystallites (and their easy axes of magnetization). The magnetization curve of $GdFe_2Al_{10}$ (Fig. 5) does not confirm the metamagnetism suspected from the field dependence of the $1/\chi$ *vs.* T plot (Fig. 4,

Table 5 Magnetic properties of the compounds $LnFe_2Al_{10}$[a]

compound	μ_{exp}/μ_B	μ_{eff}/μ_B	Θ/K	T_N/K	type of magnetism
YFe_2Al_{10}	—	—	—	—	Pauli paramagnetic
$LaFe_2Al_{10}$	—	—	—	—	Pauli paramagnetic
$CeFe_2Al_{10}$	—	2.54/0	—	—	mixed valence $Ce^{3+/4+}$, mainly 3+
$PrFe_2Al_{10}$	3.6(1)	3.58	0(10)	—	Curie–Weiss paramagnetic
$NdFe_2Al_{10}$	3.7(1)	3.62	5(5)	—	Curie–Weiss paramagnetic
$SmFe_2Al_{10}$	1.5(1)	1.66	—	14(3)	Van Vleck param., antiferrom.
$GdFe_2Al_{10}$	7.9(1)	7.94	0(5)	15(3)	metamagnetic
$TbFe_2Al_{10}$	10.0(1)	9.72	0(5)	14(3)	metamagnetic
$DyFe_2Al_{10}$	10.6(1)	10.64	0(5)	10(3)	metamagnetic
$HoFe_2Al_{10}$	10.6(1)	10.60	0(5)	<20	metamagnetic?
$ErFe_2Al_{10}$	9.5(1)	9.58	0(5)	<15	metamagnetic?
$TmFe_2Al_{10}$	7.9(1)	7.56	0(5)	<10	metamagnetic?
$YbFe_2Al_{10}$	—	0/4.54	—	—	mixed valence $Yb^{2+/3+}$

[a]The experimentally determined effective magnetic moments μ_{exp} are compared with the theoretical ones μ_{eff} for the free ions Ln^{3+} or $Ce^{3+/4+}$ and $Yb^{2+/3+}$, respectively.[29] The paramagnetic Curie temperatures (Weiss constants) Θ and the Néel temperatures T_N are also given. The values in parentheses are estimated error limits in the place values of the last listed digits.

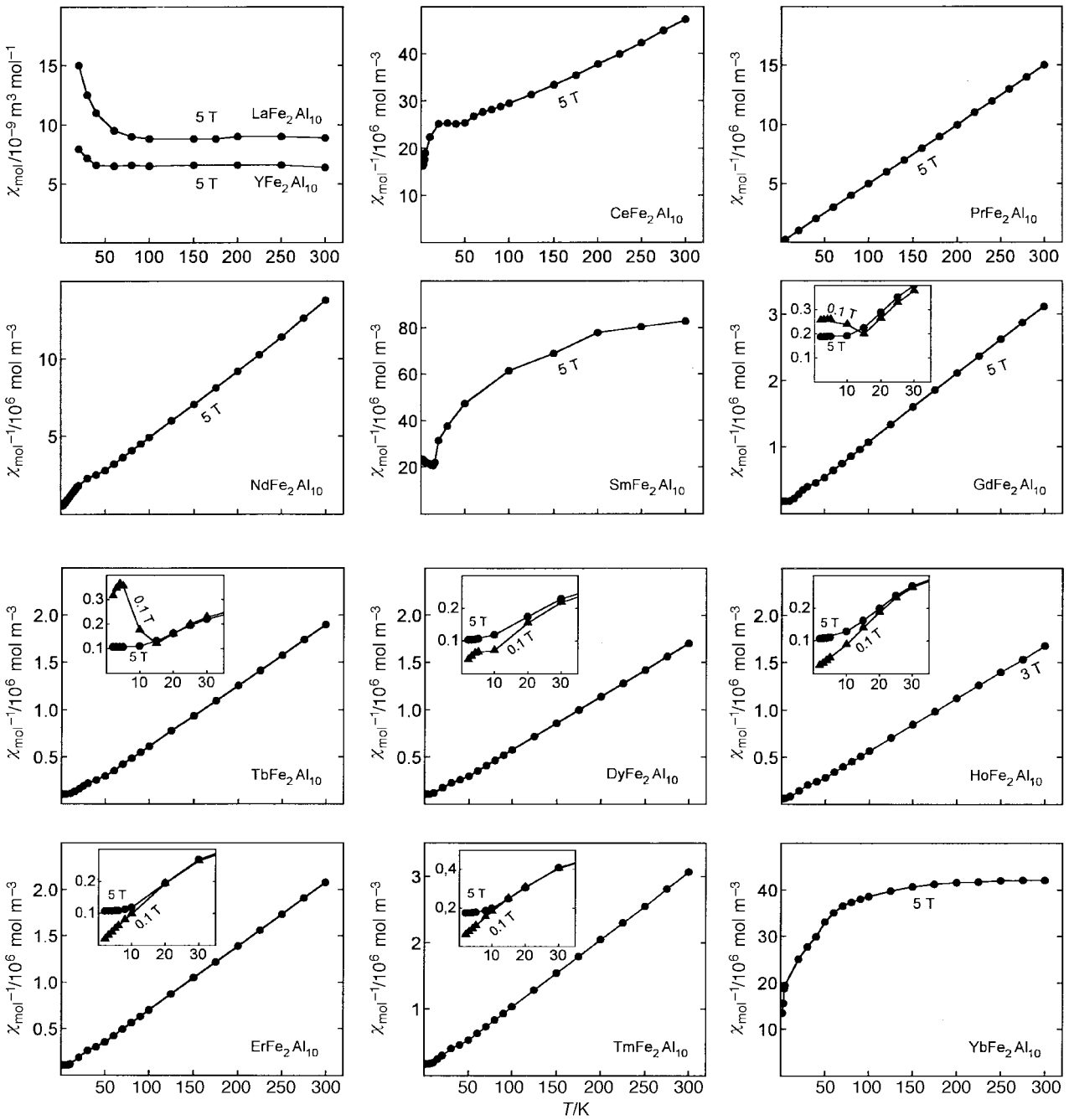

Fig. 4 Magnetic properties of the compounds $LnFe_2Al_{10}$. The magnetic susceptibilities of YFe_2Al_{10} and $LaFe_2Al_{10}$ as well as the reciprocal susceptibilities of the other $LnFe_2Al_{10}$ compounds are plotted as a function of temperature. The magnetic field strengths B are indicated. The insets show the low-temperature behaviour at various magnetic flux densities.

inset). This magnetization curve looks more like that of a regular antiferromagnet. The reason for the slight discontinuity of this curve at *ca.* 1 T was not further investigated.

The magnetic susceptibility behaviour of the three compounds $HoFe_2Al_{10}$, $ErFe_2Al_{10}$ and $TmFe_2Al_{10}$ is difficult to interpret. These compounds show similar $1/\chi$ *vs.* T plots (Fig. 4) and magnetization curves (Fig. 5). The latter look like those expected for a very soft ferromagnet. Such magnetization curves are obtained when they are recorded only a few degrees below the Curie temperature. However, the $1/\chi$ *vs.* T plots of these (zero field cooled) samples recorded with a magnetic field strength of 0.1 T do not give any indications for ordering temperatures. Possibly these compounds have an antiferromagnetic ground state and the magnetization curves should be regarded as those of a metamagnet. From the differences in the reciprocal susceptibilities recorded on heating in magnetic fields of 0.1 and 5 T (Fig. 4) we conclude that the ordering temperatures must be below 20, 15 and 10 K for $HoFe_2Al_{10}$, $ErFe_2Al_{10}$ and $TmFe_2Al_{10}$, respectively. The magnetizations at the highest attained magnetic field strengths amount to 6.9(1), 6.9(1) and 4.4(1) μ_B (Fig. 5). The theoretical values for the saturation magnetization for Ho^{3+}, Er^{3+} and Tm^{3+} are 10.0, 9.0 and 7.0 μ_B, respectively. Hence, the experimental values compare well with the theoretical ones considering that the experimental values were obtained from powder samples. Therefore, these magnetization curves cannot be ascribed to impurities.

The cell volume of $YbFe_2Al_{10}$ is larger than those of the adjacent compounds $TmFe_2Al_{10}$ and $LuFe_2Al_{10}$. This indicates mixed or intermediate $Yb^{2+/3+}$ valence. Hence, the $1/\chi$ *vs.* T curve of this compound should not be evaluated according to the Curie–Weiss law as was mentioned above for $CeFe_2Al_{10}$. Nevertheless, we have fitted these data to a modified Curie–Weiss law $\chi=\chi_0+C/(T-\Theta)$. This resulted in a temperature

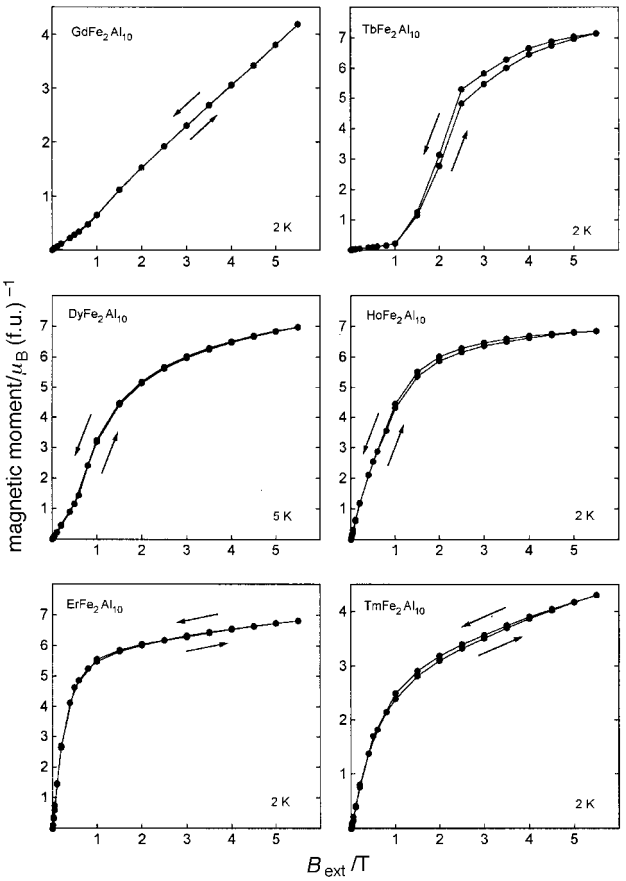

Fig. 5 Magnetization of the compounds $LnFe_2Al_{10}$ (Ln = Gd–Tm) as a function of the magnetic flux density B_{ext} measured at 2 or 5 K, respectively

independent term of $\chi_0 = 24(2) \times 10^{-9}$ m^3 (f.u.)$^{-1}$, which is about three to four times higher than the Pauli paramagnetism of YFe_2Al_{10} and $LaFe_2Al_{10}$ (see above). The magnetic moment $\mu_{exp} = 0.6(1)\ \mu_B$, obtained from the C value of this fit, is much closer to the theoretical value of $\mu_{eff} = 0\ \mu_B$ for Yb^{2+} than it is to the value $\mu_{eff} = 4.55\ \mu_B$ expected for Yb^{3+}, thus indicating ytterbium to be nearly divalent.

We thank Dipl.-Ing. U. Ch. Rodewald for the collection of the single-crystal diffractometer data and Mr K. Wagner for the work at the scanning electron microscope. We are also grateful to Dr G. Höfer (Heraeus Quarzschmelze) for a generous gift of silica tubes. This work was supported by the Deutsche Forschungsgemeinschaft and the Fonds der Chemischen Industrie.

References

1 O. S. Zarechnyuk and P. I. Kripyakevich, *Sov. Phys. Crystallogr.*, 1963, **7**, 436.
2 H. R. Kirchmayer, *Z. Metallkd.*, 1969, **60**, 699.
3 K. H. J. Buschow, J. H. N. Van Vucht and W. W. Van den Hoogenhof, *J. Less-Common Met.*, 1976, **50**, 145.
4 I. Felner and I. Nowik, *J. Phys. Chem. Solids*, 1978, **39**, 951.
5 I. Felner and I. Nowik, *Solid State Commun.*, 1978, **28**, 67.
6 I. Felner and I. Nowik, *J. Phys. Chem. Solids*, 1979, **40**, 1035.
7 W. Schäfer and G. Will, *J. Less-Common Met.*, 1983, **94**, 205.
8 W. Suski, *J. Alloys Compd.*, 1995, **223**, 237.
9 I. Felner, *J. Less-Common Met.*, 1980, **72**, 241.
10 W. Zarek and A. Winiarska, *J. Less-Common Met.*, 1988, **141**, 321.
11 P. Villars and L. D. Calvert, *Pearson's Handbook of Crystallographic Data for Intermetallic Phases*, The Materials Information Society, Materials Park, OH, 1991.
12 S. Niemann and W. Jeitschko, *Z. Kristallogr.*, 1995, **10**, 338.
13 O. S. Zarechnyuk, E. I. Emes-Misenko, V. R. Ryabov and I. I. Dikii, *Izv. Akad. Nauk SSSR, Metal.*, 1968, 219.
14 O. I. Vivchar, O. S. Zarechnyuk and V. R. Ryabov, *Izv. Akad. Nauk SSSR, Metal.*, 1970, 211.
15 V. R. Ryabov, O. S. Zarechnyuk, D. M. Rabkin and O. I. Vivchar, *Avtomat. Svarka*, 1971, **24**, 76.
16 O. S. Zarechnyuk, R. M. Rykhal, V. R. Ryabov and O. I. Vivchar, *Izv. Akad. Nauk SSSR, Metal.*, 1972, 208.
17 O. S. Zarechnyuk, O. I. Vivchar and V. R. Ryabov, *Visn. L'viv Univ., Ser. Khim.*, 1972, No. 14.
18 O. I. Vivchar, O. S. Zarechnyuk and V. R. Ryabov, *Dopov. Akad. Nauk Ukr. RSR, Ser. A*, 1973, **35**, 1040.
19 O. I. Vivchar, O. S. Zarechnyuk and V. R. Ryabov, *Dopov. Akad. Nauk Ukr. RSR, Ser. A*, 1973, **35**, 159.
20 O. I. Vivchar, O. S. Zarechnyuk and V. R. Ryabov, *Dopov. Akad. Nauk Ukr. RSR, Ser. A*, 1974, **36**, 363.
21 L. Angers, *Diss. Abstr. Intern.*, 1986, **46**, No. DA 8600847.
22 H. Klesnar and P. Rogl, *J. Mater. Res.*, 1991, **6**, 53.
23 S. Niemann, Doctoral Thesis, Universität Münster, 1994.
24 D. T. Cromer and J. B. Mann, *Acta Crystallogr., Sect. A*, 1968, **24**, 321.
25 D. T. Cromer and D. Liberman, *J. Chem. Phys.*, 1970, **53**, 1891.
26 M. Reehuis, T. Vomhof and W. Jeitschko, *J. Less-Common Met.*, 1991, **169**, 139.
27 K. Zeppenfeld, R. Pöttgen, M. Reehuis, W. Jeitschko and R. K. Behrens, *J. Phys. Chem. Solids*, 1993, **54**, 257.
28 J. Donohue, *The Structures of the Elements*, Wiley, New York, 1974.
29 S. Legvold, *Ferromagnetic Materials*, ed. E. P. Wohlfarth, North Holland, Amsterdam, 1980, vol. 1, pp. 183–295.
30 J. M. Lawrence, P. S. Riseborough and R. D. Parks, *Rep. Prog. Phys.*, 1981, **44**, 1.
31 J. H. van Vleck, *The Theory of Electric and Magnetic Susceptibilities*, Oxford University Press, London, 1932.

Paper 7/05854C; *Received* 11*th August*, 1997